On the nature of RuS$_2$ HDS active sites: insight from ab initio theory

Maria E. Grillo [a,*], Philippe Sautet [b,c]

[a] *Fritz-Haber Institut der Max-Planck Gesellschaft Faradayweg 4-6, D-14195 Berlin-Dahlem, Germany*
[b] *Institut de Recherches sur la Catalyse, 2 Av. A. Einstein, 69626 Villeurbanne Cedex, France*
[c] *Laboratoire de Chimie Theorique, Ecole Normale Superieure de Lyon, 69364 Lyon Cedex 07, France*

Abstract

The adsorption of thiophene over different hydrogenated RuS$_2$(1 1 1) defect-surface terminations has been studied using ab initio density functional theory. The highest adsorption energy is obtained for thiophene adsorbing with the molecular ring perpendicular to the surface plane (η^1-coordination) on a stoichiometric termination at a hydrogen coverage involving solely protonic SH species at the surface. However, as previously calculated for the (1 0 0) surface, this position does not seem to favor thiophene activation. The presence of surface hydrides (RuH) stabilizes the η^5-coordination through the enhanced hybridization to the thiophene C–S and C–C π-states respect to the η^1-position. The largest tendency to thiophene activation with respect to the αC–S bond breaking is obtained for a η^5-coordination on a reduced termination exposing coordinatively unsaturated Ru-atoms. In this equilibrium geometry, the thiophene-ring is centered over a hydride specie (RuH) over the sulfur vacancy. Participation of hydridic surface species in the activation process is analyzed in terms of the relative position of the density of H-s-states for both types of hydrogens at the surface. The mechanisms governing the activation are discussed based on the change of the thiophene electronic structure over interaction with the model active-surfaces. © 2001 Elsevier Science B.V. All rights reserved.

Keywords: Ab initio quantum chemical methods; Surface energy; Surface relaxation and reconstruction; Ruthenium; Sulphides; Low index single crystal surfaces; Semiconducting surfaces

1. Introduction

Over the past few years much attention has been given to study the activation of sulfur containing compounds [1]. Besides the academic interest, this tendency is due to the worldwide increasing environmental restrictions set to fossil fuel feedstocks as well as to refined oil-cuts. Consequently, the challenging task of developing more efficient hydrotreating catalysts

is posed to the refining industry. The catalytic process of sulfur removal involves both a carbon–sulfur bond cleavage (hydrodesulfurization, HDS) and hydrogenation (HYD) steps. Despite the extensive research on these processes, the general mechanistic details of HDS and HYD reactions over transition metal-sulfides have not been well understood. The standard industrial catalysts involve nickel-promoted molybdenum sulfides [2]. Although too expensive for commercial purposes, ruthenium disulfide (RuS$_2$) has proved to be the most active catalyst for HDS of thiophene among all transition metal-sulfides [3,4].

* Corresponding author. Tel.: +49-30-84134806;
fax: +49-30-84134701.
E-mail address: grillo@fhi-berlin.mpg.de (M.E. Grillo).

The mechanism of hydrogen activation over ruthenium disulfide has been the point at issue of several experimental investigations. Early works suggested a homolytic dissociation mechanism on the surface sulfur anions [1]. More recently, however, a heterolytic splitting of hydrogen on sulfur vacancies has been suggested by Lacroix and coworkers [5–7]. Studying the H_2–D_2 reaction on unsupported ruthenium disulfide catalysts after different degrees of desulfurization they found an initial increase in the exchange activity with sulfur removal. Furthermore, by means of hydrogen thermodesorption and ^1H nuclear magnetic resonance (NMR) experiments, two types of hydrogen species were characterized showing different behaviors with the degree of catalyst reduction. The amount of the low temperature hydrogen thermodesorption peak (Hd) was found to be correlated with the hydrogenation activity. These species were assigned to hydridic hydrogens chemisorbed on exposed ruthenium cations. Thus, as a result, a heterolytic hydrogen dissociation mechanism on dual sites constituted by coordinatively unsaturated metal cations (CUS) and sulfur anions was proposed.

Despite its unique HDS-activity, there is only a previous ab initio DFT-study of the thiophene interaction with ruthenium disulfide. Using the Vienna ab initio Simulation Program (VASP) [8–11], the adsorption of thiophene on $RuS_2(1\,0\,0)$ was investigated [12]. The activation was found to take place for the thiophene-ring oriented parallel to an under-stoichiometric surface termination. In the present work, the thiophene adsorption on selected $RuS_2(1\,1\,1)$ surface termination models is investigated employing the VASP code. In recent papers [13,14] we reported a comprehensive study of the atomic- and electronic-structure of several possible hydrogenated $RuS_2(1\,1\,1)$ termination models for different degrees of surface reduction. In the present study we examine the η_1 and η_5 adsorption configurations (i.e. for the molecule with the ring perpendicular or parallel to the surface) and demonstrate that the η_1-coordination corresponds to the highest adsorption energy on the stoichiometric surface. Formation of sulfur vacancies leaving coordinatively unsaturated ruthenium sites favors a parallel adsorption (η_5-coordination) and the tendency to a C–S bond activation. The present results on thiophene adsorption over selected defect-surface termination models are consistent with the experi-

mentally suggested higher activity of terminations involving both hydridic and protonic species.

2. Methodology

Based on finite-temperature DFT, the VASP code solves the Kohn–Sham equations using a plane-wave basis set. In the present calculations, an energy cut-off of 220 eV, and the exchange-correlation functional of Ceperley and Adler as parameterized by Perdew and Zunger [15] with the generalized gradient approximation [16], were used. The electron–ion interaction is described using ultrasoft pseudo-potentials [17]. The adsorption-induced surface relaxation is determined via a conjugate-gradient minimization of the total energy using the Hellmann–Feynman forces acting on the ions.

2.1. Surface models

The $(1\,1\,1)$ surface unit cell is hexagonal with four Ru- and a maximum of eight S-atoms above the ruthenium plane forming four S_2 pairs. Within a layer the sulfur atoms are, thus, distributed at four different levels (i.e. a sulfur atom of the perpendicular pair three-coordinated to the closest ruthenium plane and its corresponding topmost sulfur) and three sulfurs on near-top and bridge-sites associated to the pairs tilted to the surface normal. The asymmetric slab used to model the surfaces comprises a central sulfur sheet between two ruthenium planes surrounded by a bottom four-pair sulfur sheet, and a maximum of four surface S-atoms in the stoichiometric termination. In all calculated termination models, a vacuum thickness of 10 Å separating the slabs and a number of six special k-points in the irreducible part of the Brillouin zone were used.

In our previous study [14] we calculated the hydrogen induced surface relaxation for several surface sulfur concentrations (Θ^S) and hydrogen coverages (Θ^H) ranging from three to five atoms per unit cell. The lateral (Δx, Δy) and perpendicular (Δz) movements of the surface sulfurs, topmost ruthenium layers and inner sulfur-sheet were fully optimized, fixing the coordinates of the bottom Ru- and S-layers underneath. The equilibrium lattice constant of 5.68 Å previously determined [13] was used. In the present
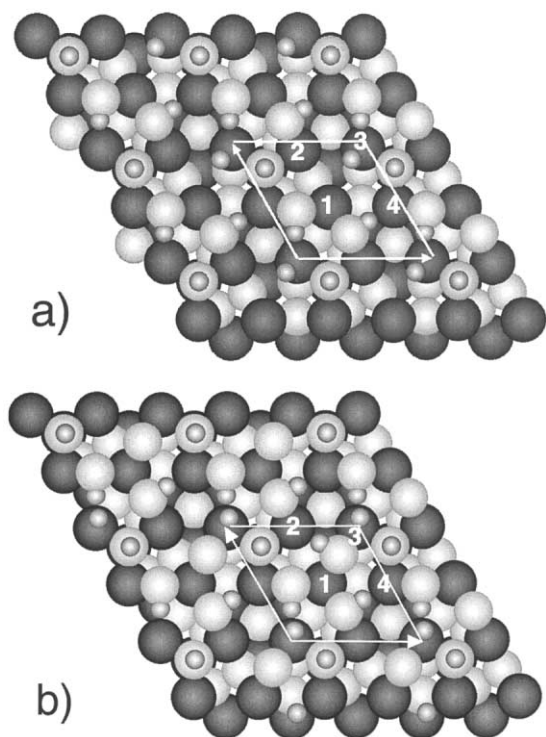
Fig. 1. Hard-sphere models for the top-views of the reduced termination 3H4 (a) with three SH and a RuH, and of the stoichiometric 4H5 (b) showing four protonic SH and a hydridic RuH specie per surface unit cell. The light colored atoms represent sulfur atoms (large) and hydrogen atoms (small). The unit cells are shown by arrows.

work, the thiophene adsorption over selected hydrogenated models for the stoichiometric and a higher reduced under-stoichiometric termination is investigated. On the former surface, hydrogen coverages (θ_H) of 4 (model 4H4) and 5 (model 4H5, Fig. 1b) atoms per surface unit cell are considered. At $\theta_H = 4$, the surface presents exclusively protonic-hydrogens (adsorbed on sulfur anions, SH), whereas at $\theta_H = 5$ there is, additionally, a H-atom adsorbed on a ruthenium site (hydride, Hd) per surface unit-cell. Particularly, the under-stoichiometric termination (model 3H4, Fig. 1a) presents hydridic species on coordinatively unsaturated ruthenium cations. Fig. 1 displays hard-sphere models for the top-views of the hydrogenated terminations 4 and 3 for hydrogen coverages of five (model 4H5) and four atoms (model 3H4) per surface unit cell, respectively.

Thiophene, H_2 and H_2S reference chemical potentials used to calculate the adsorption energies were determined with a periodic model of non-interacting molecules located at the origin of a cubic simulation box with lattice parameter of 1 nm in size and 10 k-points for the Brillouin zone integrations. The geometric and electronic structures calculated for thiophene compare well with the experimental bond lengths and reported vertical ionization potentials [19]. The bond distances were reproduced within a precision of 0.01 and 0.02 Å for C–C, C–S and C–H bonds, respectively.

3. Results and discussion

3.1. Thiophene chemisorption on RuS$_2$(1 1 1) surfaces

The obtained adsorption energies for the thiophenic-ring oriented perpendicular (η_1-coordination via the S-atom) and parallel (η_5-coordination) to the surface plane are listed in Table 1 for the considered hydrogenated termination models. In both η_1- and η_5-coordination modes, the thiophenic sulfur is located in the hollow site formed by the ruthenium atoms 1–3 as shown in Fig. 1. For the flat-adsorption (η_5), the thiophenic ring is positioned along the bridge between the Ru-atoms 1 and 2 (Fig. 1), with the C_β–C_β bond axis rotated 30° with respect to the rutheniums 1 and 4 in Fig. 1. In each case, the complete thiophene molecule as well as the surface-hydrogens, -sulfurs and -ruthenium atoms were allowed to relax, until convergence of the Hellmann–Feynman forces.

The perpendicular adsorption geometry (η_1) turns out to be energetically preferred over the parallel

Table 1
Calculated adsorption energies for perpendicular (η_1) and parallel (η_5) orientations of the thiophenic ring respect to the surface plane on the considered hydrogenated termination models[a]

Termination model	Θ^S	Θ^H	η_1	η_5
4H5	4	5	−0.99	−0.96
4H4	4	4	−0.75	−0.61
3H4	3	4	−0.80	−0.83

[a] Θ^H and Θ^S refer to the surface hydrogen- and sulfur-coverages. The surface termination models are labeled according to the number of hydrogen and sulfur atoms per unit cell. The energies are given in eV per cell.

orientation (η_5) in the stoichiometric termination (model 4H4) at a hydrogen coverage of four atoms per surface unit cell ($\Theta^H = 4$). Whereas, the energy difference between both adsorption modes (η_5 and η_1) is smaller on the surface models presenting hydridic species on Ru-sites (models 4H5 and 3H4). Indeed on the under-stoichiometric termination model 3H4, parallel thiophene adsorption is slightly more stable than the perpendicular-geometry (η_1). This is expected from the lower steric hindrance approaching the surface of lower Θ^S (i.e. lower Pauli repulsion). As a consequence, in the equilibrium configuration bond distances between the thiophenic α- and β-hydrogens to surface sulfurs of 2.37 and 3.06 Å on model 3H4 compared to 3.56 and 3.62 Å on model 4H4 are calculated. This points to a stronger hybridization of the thiophenic ring in η_5 orientation to the surface at a lower sulfur coverage.

The predicted preference for η_5 over η_1 on the reduced termination model 3H4 is consistent with previous VASP-results for thiophene adsorption on $MoS_2(0\,1\,0)$ [18]. Indeed similar to that study, the equilibrium η_5-configuration is tilted about the C_α–C_β axis (see Fig. 2) with a closest thiophene distance to the surface of 2.37 Å between a α-hydrogen and a surface-S (compared to 2.84 Å on model 4H5), and a hydride distance to the nearest thiophenic C_α-atom of 2.83 Å (compared to 3.01 Å on model 4H5).

The highest adsorption energies on termination models presenting surface hydrides (models 3H4 and 4H5) were obtained for parallel positions in which the thiophenic-ring is centered above the hydridic
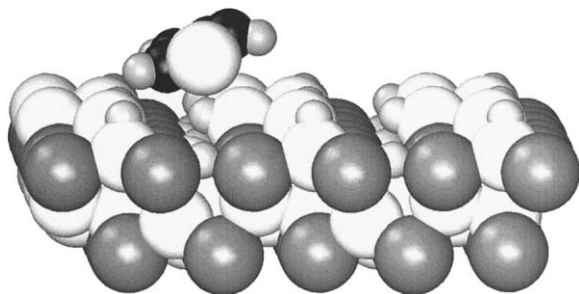

Fig. 2. Graphical representation of a side-view of the equilibrium thiophene configuration for parallel adsorption (η_5) on the reduced termination model 3H4. The light colored atoms represent sulfur atoms (large) and hydrogen atoms (small), and the dark spheres represent the carbons.
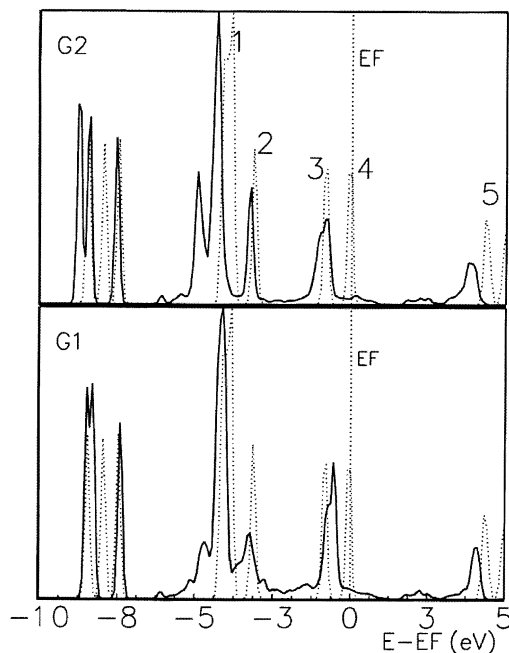

Fig. 3. Local electronic density of states (DOS) for a free (dashed lines) and for thiophene interacting with the termination model 3H4 ($\Theta^S = 3$, $\Theta^H = 4$) in η_5 (G2, top panel) and η_1 (G1, bottom panel) adsorption geometries, respectively. The labels numbering the free-thiophene features are referred in the text. The DOS (states/eV atom) are displayed for energies relative to the Fermi level ($E - E_F$).

specie on a Ru-site (see Fig. 2 for model 3H4). Participation of thiophenic-π-states to the bonding in η_5 on these surfaces can be discussed in terms of the surface induced changes in the density of states (DOS) for adsorbed thiophene compared to the free molecule (see Fig. 3). The labeled features in Fig. 3 represent bonding C–C and S–C π-states (band 1), sulfur-lone pair (band 2), bonding C_β–C_β and S–C π-states (band 3), bonding C_α–$C_\alpha\pi$-states (band 4), and the lowest unoccupied anti-bonding C–S-π states (band 5). Contribution of the bonding C–C and S–C π-states (band 1) to the interaction with surface hydrides might be inferred by the shift and splitting of this band on the termination model 3H4 for thiophene in the η_5 orientation compared to η_1, see Fig. 3.

In the most favorable adsorption system, (i.e. η_1 orientation on termination 4H5, see Table 1), the thiophene molecule is tilted with respect to the surface normal coordinating via the sulfur atom (at 2.63 Å to

Table 2
Percentual changes of the thiophene bond lengths upon η_5 adsorption on the considered surface models with respect to the gas-phase thiophene structure

Θ^S	Θ^H	S–C	C_α–C_β	C_β–C_β
4	5	0.40	0.30	0.14
4	4	0.10	1.50	1.00
3	4	0.60	0.80	0.90

its nearest surface protonic-H) and H_α-atom (at 2.84 Å to its closest surface-S). Using the same code as in the present study [12], similar equilibrium geometries on the bare stoichiometric and reduced $RuS_2(1\,0\,0)$ surface terminations were obtained. Nonetheless, on the $(1\,0\,0)$-plane significantly lower adsorption energies of 0.43 and 0.10 eV, respectively, compared to the present $(1\,1\,1)$ surface terminations (Table 1) were calculated.

Similarly to the thiophene adsorption over a $RuS_2(1\,0\,0)$ surface, there is no sign of activation on the most stable adsorption geometry over the $(1\,1\,1)$ plane. Additionally, in agreement with the adsorption on $MoS_2(0\,1\,0)$ [18], the largest differences in the thiophene bond lengths after interaction with the surface are obtained in η_5-coordination. Moreover, comparing the percentual changes of the thiophene bond lengths upon η_5 adsorption on the considered surface models with respect to the free-thiophene structure (Table 2), the largest increase of the C–S bond length is calculated on the reduced model 3H4. Whereas, the most pronounced changes in the C_α–C_β and C_β–C_β bond lengths are obtained on the stoichiometric surface model 4H4. This might indicate that the largest tendency to C–S bond activation (HDS) appears to be obtained on a coordinatively unsaturated Ru-site with the thiophenic-ring centered over a hydride specie (termination 3H4), and a stronger tendency to activate the C–C bonding (HYD) on the more saturated surface model (termination 4H4).

3.2. Electronic factors

The distinct mechanisms of interaction in the two different coordination modes, η_5 and η_1, may be examined in terms of the relative positions of the DOS projected on the protonic- (P) and hydridic-hydrogens (H) for both η_5 and η_1 adsorption geometries on termination 3H4 (Fig. 4). A striking difference in
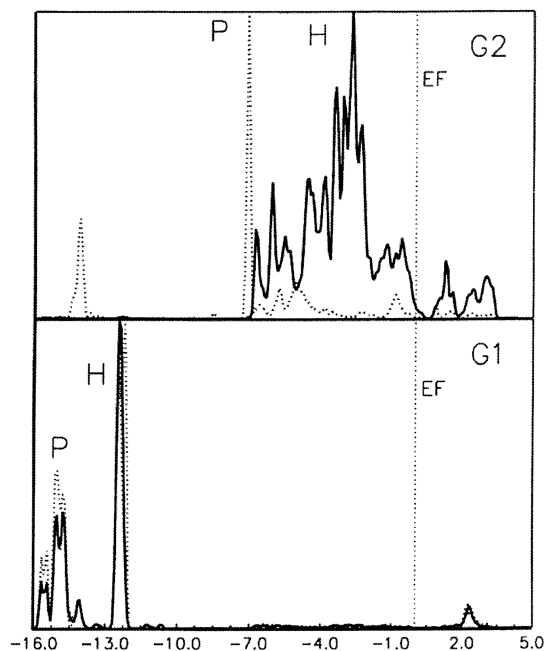

Fig. 4. Local electronic density of states (DOS) projected on the protonic (P, dashed lines) and on the hydridic (H) hydrogens of the reduced surface model 3H4 ($\Theta^S = 3$, $\Theta^H = 4$). The top and bottom panels show the DOS for thiophene adsorbing in η_5 (G2, see Fig. 2) and η_1 (G1) modes, respectively. The DOS (states/eV atom) are displayed for energies relative to the Fermi level ($E - E_F$).

the position of the hydride-s-states for the two adsorption geometries is observed (see Fig. 4). For the thiophenic-ring lying parallel (G2 in Fig. 4) to termination 3H4, the hydridic-s-states form a bonding wide band below E_F resulting, in particular, from the hybridization to bonding S–C_α-π and C_β–C_β-π states (band 1 in Fig. 4) and to the C_α–C_α states (band 4 in Fig. 4). In contrast in the perpendicular adsorption mode both protonic and hydridic s-states are localized at high binding energies and practically do not contribute to the thiophene bonding (see Fig. 4).

4. Conclusions

In summary, the present ab initio study sheds some light into the role of coordinatively unsaturated Ru-vacancies in the interaction with thiophene. We demonstrate that the parallel η_5-interaction is stabilized by a stronger thiophene hybridization to surface

hydrides on exposed Ru-sites compared to a perpendicular η_1 thiophene coordination to the surface. This adsorption geometry seems also to favor C–S bond activation, as already found for $RuS_2(1\,0\,0)$ and $MoS_2(0\,1\,0)$ surfaces. The present results confirm the experimentally observed correlation between the concentration of hydrogen species adsorbed on coordinatively unsaturated ruthenium cations with the hydrogenation catalytic activity for unsupported ruthenium-sulfide catalysts found by Lacroix and coworkers.

Acknowledgements

References

[1] H. Topsøe, B.S. Clausen, F.E. Massoth, Hydrotreating Catalysis-Science and Technology, Springer, Berlin, 1996, p. 209.
[2] B.C. Gates, J.R. Katzer, G.C. A. Schuit, Chemistry of Catalytic Processes, McGraw-Hill, New York, 1980.
[3] M. Lacroix, N. Boutarfa, C. Guillard, M. Vrinat, M. Breysse, Catalysis 120 (1989) 473.
[4] M. Lacroix, H. Marrakchi, C. Calais, M. Breysse, C. Forquy, in: M. Guisnet (Ed.), Heterogeneous Catalysis and Fine Chemicals II, Elsevier, Amsterdam, 1991, p. 277.
[5] M. Lacroix, S. Yuan, M. Breysse, C. Doremieux-Morin, J. Fraissard, J. Catal. 138 (1992) 409.
[6] H. Jobic, C. Clugnet, M. Lacroix, S. Yuan, C. Mirodatos, M. Breysse, J. Am. Chem. Soc. 115 (1993) 3654.
[7] M. Breysse, C. Geantet, M. Lacroix, J.-L. Portefaix, M. Vrinat, in: M.L. Occelli, R. chianelli (Eds.), Hydrotreating Technology for Pollution Control, Marcel Dekker, New York, 1999.
[8] G. Kresse, J. Hafner, Phys. Rev. B 47 (1993) 5858.
[9] G. Kresse, J. Hafner, Phys. Rev. B 49 (1994) 14251.
[10] G. Kresse, J. Furthmüller, Comput. Mater. Sci. 6 (1996) 15.
[11] G. Kresse, J. Furthmüller, Phys. Rev. B 54 (1996) 11169.
[12] V. Smealyansky, J. Hafner, G. Kresse, Phys. Rev. B 58 (1998) R1782.
[13] M.E. Grillo, V. Smelyansky, P. Sautet, J. Hafner, Surf. Sci. 439 (1999) 163.
[14] M.E. Grillo, P. Sautet, Surf. Sci. 457 (2000) 285.
[15] J.P. Perdew, A. Zunger, Phys. Rev. B 23 (1981) 5048.
[16] J.P. Perdew, J.A. Chevary, S.H. Vosko, K.A. Jackson, M.R. Pederson, D.J. Singh, C. Fiolhais, Phys. Rev. B 46 (1992) 6671.
[17] D. Vanderbilt, Phys. Rev. B 41 (1980) 7892.
[18] P. Raybaud, J. Hafner, G. Kresse, H. Toulhoat, Phys. Rev. Lett. 80 (1998) 1481.
[19] P.J. Derrick, L. Åsbrink, O. Edqvist, B.-Ö. Jonsson, E. Lindholm, Int. J. Mass Spectrom. Ion Phys. 6 (1971) 177.